Fluidization of Coated Group C Powders

Yuhua Chen, Jun Yang, Rajesh N. Dave, and Robert Pfeffer
New Jersey Center for Engineered Particulates (NJCEP), New Jersey Institute of Technology, University Heights, Newark, NJ 07102

DOI 10.1002/aic.11368
Published online December 4, 2007 in Wiley InterScience (www.interscience.wiley.com).

While it is well known that flow aids such as fumed silica can be added to improve flowability and fluidizability of cohesive powders, the improvements observed depend on how well the flow aids are blended together with the cohesive powders. In this work, dry particle coating is used to deposit a very small amount of nano-sized particles (as low as 0.01 wt %) with a high degree of precision onto the surface of cohesive, Geldart Group C powders to make them fluidize like Group A powders. A model taking into account the effect of the size of the guest and host particles as well as surface area coverage (SAC) of the coated nano-sized particles is developed to predict the effect of coating on the adhesion reduction of cohesive powders. A series of experiments are performed to investigate the improvement in the fluidizability of dry particle coated Group C powders (e.g., cornstarch and aluminum), and the effect of various parameters such as SAC, guest particle size and host particle size are systematically investigated. The results clearly show the effect of each of these parameters on the fluidization behavior of cohesive powders, and also validate the model. The study also indicates that a critical SAC is required to make the coated cornstarch fluidize, which is about 5%; the smaller the guest size, the better its effect on improved fluidizability, although the improvement is reduced if the guest size is smaller than about 10 nm; and if the conditions regarding the SAC and guest size are satisfied, dry particle coating will significantly improve the fluidization of cohesive particles even as small as 5–10 μm. © 2007 American Institute of Chemical Engineers *AIChE J,* 54: 104–121, 2008
Keywords: cohesive powders, fluidization, Geldart classification, dry coating, adhesion force, cohesion reduction

Introduction

Fluidized beds are widely used in many powder processes because of their continuous powder handling ability and excellent gas–solid contacting, which results in high heat and mass transfer coefficients and high rates of reaction. However, particles with different physical properties have very distinct fluidization behaviors as shown by Geldart,[1] who based on empirical observations, classified powders into four groups: A, B, C, and D, depending on their size and the density difference between the solid particles and the fluidizing medium. The objective of this article is to improve the fluidization quality of Geldart Group C powders, which normally are extremely difficult to fluidize and generally will form cracks, channels or "rat holes" or even lift as a solid plug when exposed to the fluidizing gas. The difficulty in fluidizing Group C powders is attributed to the large interparticle forces arising mainly from Van der Waals attraction, which can be up to a million times greater than the force of gravity when the particle size goes down to a few microns resulting in fine particles forming agglomerates.[2]

Past research indicates that agglomerate fluidization may be possible for Group C particles when mostly mono-sized agglomerates are formed. However, the agglomerates formed during fluidization are weak and very unstable and result in partial fluidization or even defluidization. To improve the stability of the fluidization of cohesive Group C particles, external forces may be employed, such as vibration, centrifugal

Correspondence concerning this article should be addressed to R. N. Dave at dave@adm.njit.edu.

force, magnetic assistance, acoustic and electric fields, or by addition of inert large sized particles.[3–8] These approaches have some merits, but due to the need for external excitations or addition of other materials (such as magnets) within the bed, pose practical limitations, and may hinder or interfere with subsequent powder processing such as film coating, granulation, etc.

In this study, we have used an innovative dry particle coating technique[9] to coat the cohesive powders with nanoparticles rather than blending the two powders together, and systematically studied the effect on fluidization. Dry particle coating is introduced to reliably improve the fluidization behavior of Group C cohesive particles, because it allows for depositing a very small amount of nano-sized particles with high degree of precision onto the surface of cohesive powders, thus reducing the cohesion force between fine particles. While it is well known that flow aids such as nano-sized fumed silica can be added to improve the flowability and fluidizability of cohesive powders, the improvements observed depend on how well the flow aids are blended together with the cohesive powders. In addition, there are differing opinions regarding the mechanism of improvement in fluidization due to the additives. Most researchers believe that the fine additives act as spacer particles[10–12], while some believe that there is a "ball-bearing" or lubricant effect,[13,14] and some have even proposed that nano-additives may cause neutralization of electrostatic charges.[15]

While most articles indicate that the amount of nano-additives required to obtain improvement in fluidization is about 0.5–1 wt %, very few articles clearly demonstrate the important role of surface area coverage (SAC) and/or the uniformity of coverage. An exception to this is work by Valverde et al.,[16,17] where the fluidization behavior of well-blended toner particles with fumed silica have been investigated using an innovative apparatus called the Sevilla powder tester (SPT). The SPT is a fully automated device and couples vibrations to initiate fluidization when the powders are very cohesive; e.g., nano-additive amounts are low and/or the host powders are very fine (less than 10 μm). They found that the blended fine powders exhibit solid-like, fluid-like, and bubbling regimes; where the range of velocities over, which fluid-like regime exists is logarithmically proportional to the particle Bond number, defined as the ratio of interparticle attractive force to particle weight, and shrinks to zero when Bond number is very small ($\sim$10).

In contrast to most of the reported literature, previous work by our Group[18] found that only a very small amount of nanoparticles, e.g., less than 0.1 wt %, are required as additives to significantly improve cohesive particle flowability with a high-degree of reliability, when dry particle coating is used to attach nano-particles uniformly on the surface of cohesive particles. The advantage of dry coating over simply blending the cohesive powder with the nano-particles, as reported in most articles, is that the SAC obtained for the same amount of additives is significantly higher and more uniform when using dry coating when compared with conventional blending. In this work, the dry coating approach is utilized to improve the fluidizability of cohesive Group C powders by creating a nanoscale roughness onto the powder surface.

We will first develop a new model, which builds upon the classical Rumpf model, to take into account the effect of SAC to predict the influence of coating on adhesion of cohesive powders. This allows gaining an insight into the main mechanism of cohesion reduction. Next, the efficacy of the dry coating approach to achieve a high degree of deagglomeration of nano-additives and hence improved surface coverage is illustrated. This is followed by a series of experiments to investigate the improvement in the fluidizability of Group C powders (e.g., cornstarch and aluminum) by dry particle coating them with a small amount of nano-sized particles. The experimental study examines the effect of various parameters such as, SAC, guest particle size and host particle size, and the results are compared with the proposed model.

Reduction of Cohesion Force Through Dry Coating of Nano-Additives

Particle adhesion is the result of forces such as van der Waals forces, capillary forces, electrical forces, electrostatic image forces, and chemical forces. Under normal experimental conditions, i.e., in the absence of a high-voltage field and/or liquids or vapors, and at close distances between contiguous inert particles, van der Waals adhesion forces are the dominant interparticle forces. The adhesion force between two particles is influenced by particle size, shape, surface roughness, work of adhesion, and surface free energy, material properties such as hardness and elasticity and deformation of the materials.[19]

Currently, there are three main methods to reduce adhesion forces between solid surfaces in contact[19]: adhesion force reduction by immersion of the solid sample in a liquid, adhesion force reduction due to double layer interaction, and particle removal through use of detergents. However, none of these are practical for dry powder handling. According to the Hamaker theory, the cohesion force between particles can be manipulated by altering the surface roughness (asperity) of particles. Massimilla and Donsi[20] pointed out that the cohesive force is reduced by about two orders of magnitude if the surface roughness rather than the size of the particle is taken into account; therefore the expected cohesive force has a wide range due to the size and distribution of the surface asperities.

The focus of this work is to create nano-scale surface roughness that results in cohesion reduction[21,22] through dry particle coating of nano-additives onto the surface of the carrier particles. Dry particle coating[9] is a novel process to alter the surface properties and/or functionality of fine particles by placing small, nano-size particles on cohesive particle surfaces. This process is very different from conventional blending of nano-additives with cohesive powders because it creates intimate contacts between individual and small ensembles of nano-particles with the surface of the larger, otherwise cohesive particles. The adhesion force between the smaller nano-additives and the larger host particle is significantly larger than the weight of the smaller particle, and hence it is very difficult to remove the smaller particle from the larger one during normal handling and processing.[9] A cartoon of the dry particle coating process is shown in Figure 1.

Current adhesion force models for particles with rough surfaces

Several models have been proposed to calculate the adhesion force of fine particles such as the Johnson–Kendall–

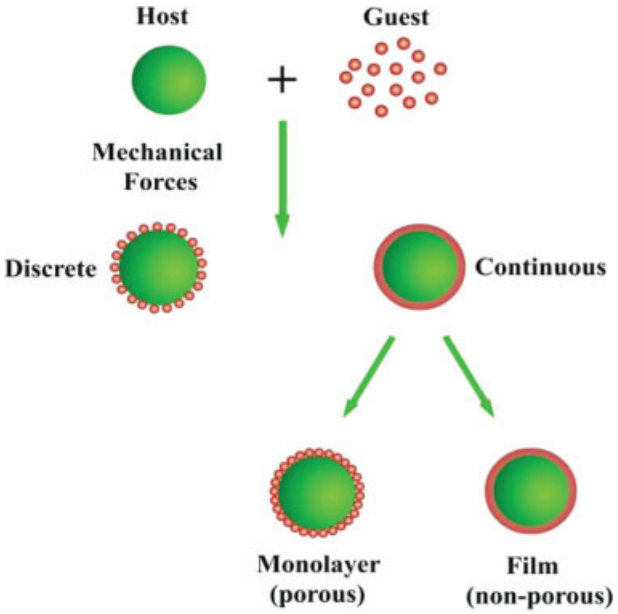

Figure 1. 1 Sketch of dry particle coating.

[Color figure can be viewed in the online issue, which is available at www.interscience.wiley.com.]

Roberts (JKR)[23] model, the Deryaguin–Muller–Toporov (DMT)[24] model and their modified/extended versions.[19] They are derived based on the deformation of the contacting surfaces. The JKR model is useful for very soft and low surface free energy materials, while the DMT model is more suitable for rigid and high surface free energy materials. However, the direct influence of surface roughness on the cohesion force is generally unaccounted for in all these models.

There are several models considering the effect of asperity on the adhesion force. Rumpf[11] modeled the adhesion between a sphere and a flat rough surface to represent the contact of a single asperity, centered on the flat rough surface, with a much larger sphere as shown in Figure 2. The Rumpf model is represented by Eq. 1. The first term represents the interaction of the large sphere in contact with the asperity and the second describes the "noncontact" force between the large sphere and the flat surface separated by the asperity.

$$F_{ad} = \frac{A}{12z_0^2}\left[\frac{dD}{d+D} + \frac{D}{(1+d/2z_0)^2}\right] \tag{1}$$

Here, A is the Hamaker Constant, $z_0 \approx 4 \times 10^{-10}$ m is the distance between two contact surfaces, d and D are the diameters for the semispherical asperity and the large sphere, respectively.

Xie[12] attempted to explain the adhesion force between two rough particles by assuming the asperity is a small particle located between the large particles (Figure 3). This model, as represented by Eq. 2, consists of the attraction between two large particles and the cohesion between the small particle and large particles. The calculation results indicate that it is the surface asperities, not the parent particles, which dominate the van der Waals forces when the surface asperities are

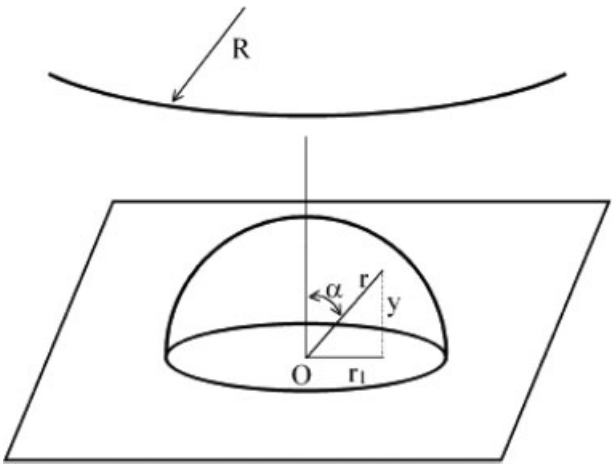

Figure 2. Schematic illustration of the Rumpf model.[21]

of the order 0.1 μm and have a negligible effect when the surface asperities are less than 10 nm.

$$F_{ad} = \frac{AD}{12(2z_0+d)^2} + \frac{A(D_1'+D_2')}{12z_0^2} \tag{2}$$

where, $D = (D_1D_2)/(D_1+D_2)$, $D_1' = (D_1d)/(D_1+d)$, and $D_2' = (D_2d)/(D_2+d)$ are characteristic diameters.

A simple model used to calculate the adhesion force between two coated particles was proposed by Mei et al.[25] On the basis of the JKR theory, this model includes the effect of the particle coating on the force-displacement relationship due to surface energy and elastic deformation. A schematic illustration of Mei's model is shown in Figure 4. The model as described by Eq. 3 indicates that the adhesion force ratio of a coated particle to an uncoated particle is proportional to the ratio of twice the guest particle radius to the host particle radius.

$$\frac{P_{coated}}{P_{uncoated}} = \frac{2R_f}{R_1} \tag{3}$$

Here, P_{coated} is the adhesion force between coated particles, $P_{uncoated}$ is the adhesion force between uncoated particles, R_f is the radius of the guest particle, and R_1 is the radius of the host particle.

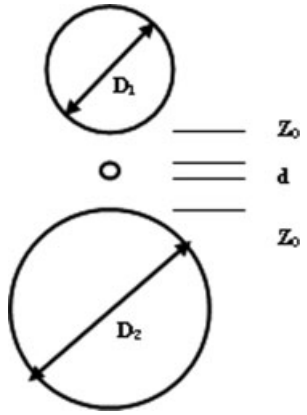

Figure 3. Illustration of sandwich contacting system.

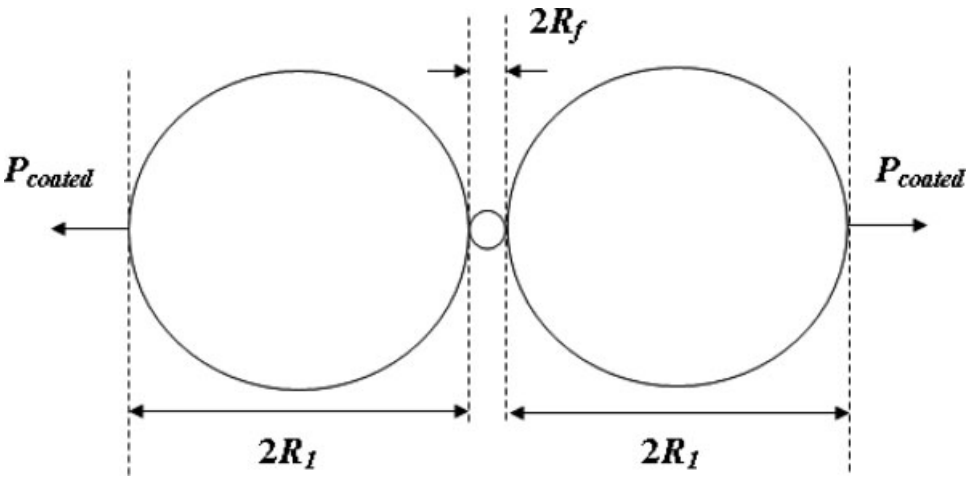

Figure 4. Schematic illustration of Mei's model.

The same result, i.e., Eq. 3 can be obtained more easily through manipulation of Rumpf's model given by Eq. 1 as was done in Yang et al.,[18] where R_1 is either the radius of the host particle or the radius of the asperities (generally taken to $\sim$0.2 μm) depending on the size of the host particles. This assumes that the Hamaker constants of both host and guest materials are approximately the same.

Rabinovich et al.[21] modified the Rumpf model by employing the root-mean-square (rms) roughness to replace the radius of a single asperity. Thus, the cohesion force between a particle and a rough surface can be expressed as

$$F_{\mathrm{ad}} = \frac{AD}{12z_0^2}\left[\frac{1}{1 + D/(2 \times 1.48\ \mathrm{rms})} + \frac{1}{(1 + 2 \times 1.48\ \mathrm{rms}/2z_0)^2}\right] \tag{4}$$

Here, rms = $0.673r$ is the root-mean-square roughness of the surface, D is the sphere diameter, and r is the radius of the asperity.

Proposed adhesion force model for coated particles

As stated in the previous section, current models mainly deal with the adhesion between two particles (surfaces) with a single small particle/asperity located between them without considering the effect of SAC of the small particles on the large particles, although the Rabinovich model goes into more details into the nature of the surface roughness. To get an estimate of the influence of SAC, we need to go beyond the simple contact configuration shown in Figure 4. For this purpose, we consider the case of three small particles supporting the two spherical host particles stably as shown in Figure 5a. Here, it is assumed that the individual guest particles are evenly coated on the host particle surface and all guest particles are monosized spheres. This is a fair assumption for dry particle coating, but is not valid for conventional blending. The three guest particles are assumed to be placed on the vertices of an equilateral triangle between the two host spheres as illustrated in Figure 5b.

The radius of the contact circle can be derived as

$$R^2 = \left(\frac{D+d}{2}\right)^2 - \left(\frac{D+H_0}{2}\right)^2 \tag{5}$$

and the area of the triangle formed by the three guest particles is

$$S = \frac{3\sqrt{3}}{4}R^2. \tag{6}$$

The number of guest particles coated on the host particle can be expressed in terms of S as

$$N = \frac{\pi D^2}{2S} = \frac{2\sqrt{3}\pi D^2}{9R^2} \tag{7}$$

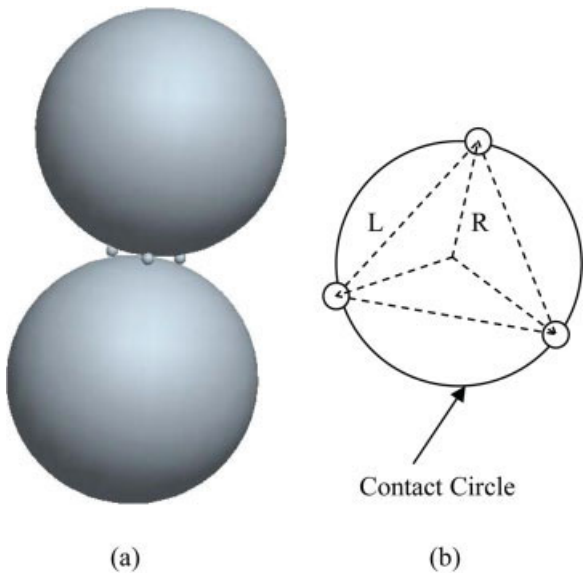

Figure 5. (a) Contact of two-coated cohesive particles and (b) Location of guest particles.

[Color figure can be viewed in the online issue, which is available at www.interscience.wiley.com.]

The SAC is then calculated as

$$\mathrm{SAC} = \frac{N \times \frac{\pi d^2}{4}}{4\pi\left(\frac{d+D}{d}\right)^2} \times 100\% = \frac{N \times d^2}{4(d+D)^2} \times 100\% \approx \frac{N \times d^2}{4(D)^2} \times 100\% \quad (8)$$

This implies that the weight percentage of the guest particles is

$$\mathrm{Wt}\ \% = \frac{(Nd^3\rho_\mathrm{d})}{(D^3\rho_\mathrm{D}) + (Nd^3\rho_\mathrm{d})} \times 100\% \quad (9)$$

According to Rumpf and Xie's models,[11,12] the adhesive force between two rough particles consists of two terms; the adhesion between large particles and the attraction between the asperity and the large particle. Similarly, the adhesive force between two coated particles can be calculated by

$$F_\mathrm{ad} = \frac{A}{12z_0^2}\left[\frac{3dD}{d+D} + \frac{D}{2(H_0/z_0)^2}\right] \approx \frac{Ad}{4z_0^2} + \frac{AD}{24H_0^2} \quad (10)$$

On the basis of Eqs. 5–8, the relationship among host–host distance H_0, host particle size D, guest particle size d, and SAC can be derived as $H_0 = \sqrt{(D+d)^2 - \frac{1.21}{\mathrm{SAC}}d^2} - D$.

Substituting H_0 in Eq. 10 by SAC, the adhesion force can be expressed in terms of SAC, guest particle diameter (d) and host particle diameter (D) as

$$F_\mathrm{ad} = \frac{Ad}{4z_0^2} + \frac{A}{24\left(\sqrt{\left(1+\frac{d}{D}\right)^2 - \frac{1.21}{\mathrm{SAC}}\left(\frac{d}{D}\right)^2} - 1\right)^2 D} \quad (11)$$

In Eqs. 5–11, A is the Hamaker constant, D is the diameter of host particle, d is the diameter of guest particle, Z_0 is the default distance between two surfaces in contact, H_0 is the distance between two coated host particles, ρ_d is the density of guest particles and ρ_D is the density of host particles. S and R are the area and radius of the contact circle, respectively, and N is the number of guest particles coated on the surface of each host particle.

Figure 6 shows the relationship between adhesion force and SAC for a cohesive particle with typical values used in the experiments; $D = 15 \times 10^{-6}$ m, $A = 10^{-19}$ J, $z_0 = 0.4$ nm, and $d = 20 \times 10^{-9}$ m. Initially the adhesion force remains unchanged, and then the adhesion force decreases abruptly with an increase of SAC, followed by the adhesion force decreasing gradually and becoming constant again. That occurs because at very low surface coverage, the guest particles do not have any effect on the adhesion force reduction because the space between neighboring guest particles on the surface of the respective host particles is so large that the host particles contact each other directly. As the concentration of guest particle increases, the direct contact and hence adhesion force between primary host particles is reduced. As can be seen in the figure, beyond a certain threshold the SAC is sufficient to prevent direct contact between two host particles. In that case, the adhesion between the two host particles is negligible compared with the adhesion between the host and guest particles, and hence, given all other conditions being constant, one cannot further reduce the cohesion by increasing the SAC.

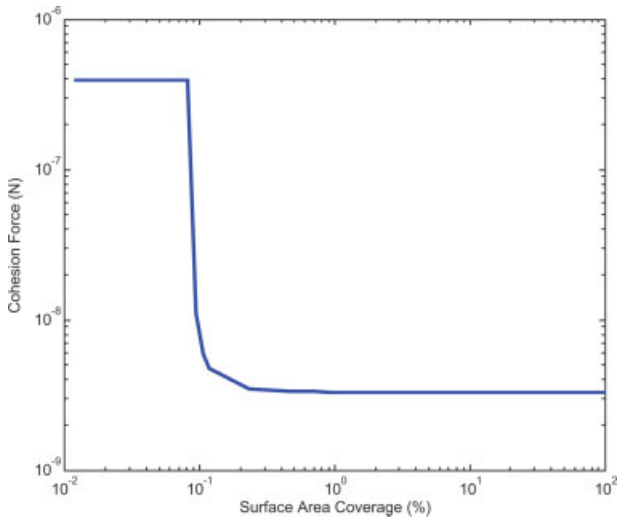

Figure 6. Cohesion force vs. surface coverage.

Host particle size $D = 15 \times 10^{-6}$ m, Hamaker constant $A = 10^{-19}$ J, distance between two contact particles $z_0 = 0.4$ nm and guest particle size $d = 20 \times 10^{-9}$ m. [Color figure can be viewed in the online issue, which is available at www.interscience.wiley.com.]

The influence of the guest particle size is examined as shown in Figure 7 for a cohesive host particle of $D = 15 \times 10^{-9}$ m, $A = 10^{-19}$ J, $z_0 = 0.4$ nm, and SAC = 100%. As seen, there exists a minimum adhesion force, which implies that the noncontact force (the cohesive force between the two noncontacting host particles) provides the primary contribution to the total adhesion force when the guest particle size is less than 8 nm for the example considered. It is noted that host–host attraction decreases with increasing guest particle size, while the host–guest force increases. These two opposing factors contribute to the minimum of the adhesion force with changing guest particle size.

Finally, the influence of the host particle size is examined as shown in Figure 8. In this case, $A = 10^{-19}$ J, $z_0 = 0.4$ nm, SAC = 100%, and $d = 10 \times 10^{-9}$ m. It can be seen that the adhesion force for coated particles with full SAC or 100% SAC (see an illustrative sketch in Figure 9) increases gradually as the host particle size increases.

Criterion for the Transition Between Group A and Group C Particles

Nase et al.[26] found by numerical simulation and experiments that the flowability of cohesive powders decreases when the granular bond number $Bo_\mathrm{g} = F_\mathrm{t}/W$ increases. Here, F_t is the inter-particle adhesion force and W is the particle weight. The granular Bond number Bo_g can be used as the criterion of transition from free-flowing particle ($Bo_\mathrm{g} < 1$) to cohesive particles ($Bo_\mathrm{g} > 1$). Thus a reduction in the granular Bond number can improve the flowability and fluidizability of cohesive powders. The reduction in the Bond number can be achieved by (a) reducing the inter-particle cohesion

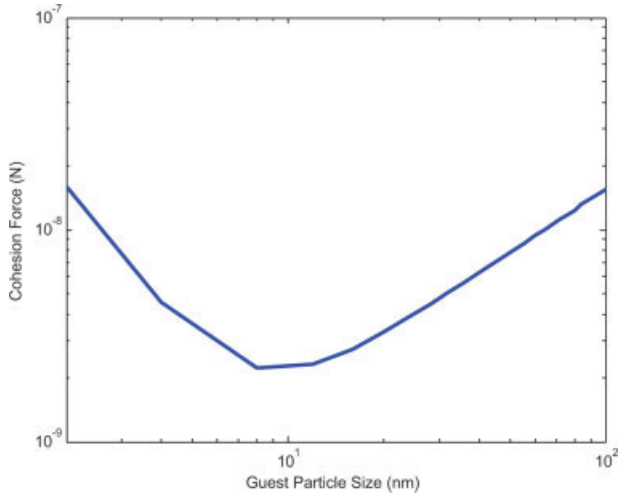

Figure 7. Cohesion force vs. guest particle size.

Host particle size $D = 15 \times 10^{-9}$ m, Hamaker constant $A = 10^{-19}$ J, distance between contact particles $z_0 = 0.4$ nm, and SAC = 100%. [Color figure can be viewed in the online issue, which is available at www.interscience.wiley.com.]

or, (b) by increasing the apparent weight of the particle by applying centrifugal force.[7] In the current work, the granular Bond number is reduced by decreasing the adhesion through dry particle coating, thus improving the fluidizability of Group C powders. This effect may be best visualized by the shift of the boundary between Geldart Group C and Group A

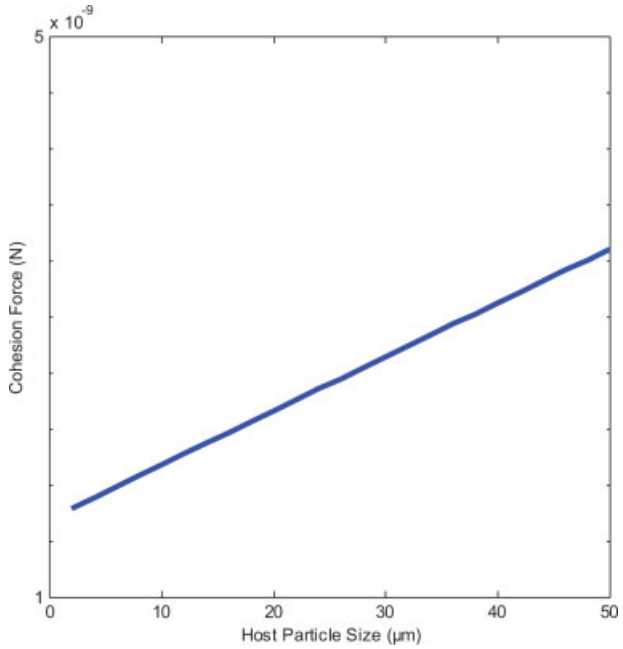

Figure 8. Cohesion force vs. host particle size.

Hamaker constant $A = 10^{-19}$ J, distance between contact particles $z_0 = 0.4$ nm, SAC = 100%, and guest particle size $d = 10 \times 10^{-9}$ m. [Color figure can be viewed in the online issue, which is available at www.interscience.wiley.com.]

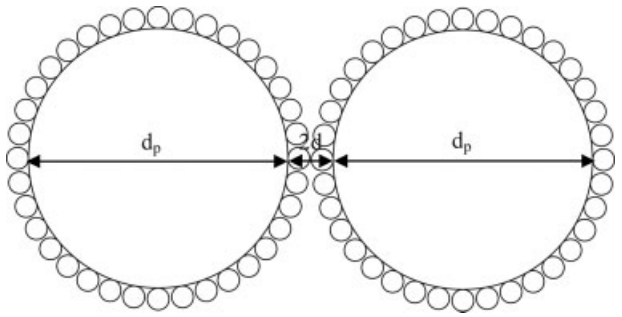

Figure 9. One possible configuration for the contact of two 100% SAC coated particles.

powders. A criterion of transition between Group C and Group A powders may be based on a semi-theoretical equation developed by Qian et al.[7]

Fluidization of cohesive powders may be considered as an equilibrium state between the drag force, gravity, buoyancy and cohesive force as shown by Eq. 12.

$$F_d = W_e + F_c \tag{12}$$

Here, F_d is the drag force of a particle in a gas–solid flow of voidage ε, W_e is the effective gravity of the particle (gravity less buoyancy), and F_c is the adhesion force between two coated particles. According to Qian et al.,[7] F_d and W_e are calculated as follows,

$$F_d = F_{ds} \times \varepsilon^{-4.8} = C_d \frac{\rho_f u^2}{2} \frac{\pi d_p^2}{4} \varepsilon^{-4.8} = \frac{\pi d_p^3}{6} (\rho_p - \rho_f) g \varepsilon^{-4.8} \tag{13}$$

$$W_e = W_g - W_b = \frac{\pi d_p^3}{6} \rho_p g - \frac{\pi d_p^3}{6} (\varepsilon \rho_f + (1 - \varepsilon) \rho_p) g = \frac{\pi d_p^3}{6} (\rho_p - \rho_f) g \varepsilon \tag{14}$$

Equation 14 in Qian et al.[7] was based on using the density of the fluidized bed to obtain the buoyancy force as originally suggested by Foscolo and Gibilaro.[27] It has come to the attention of the authors that it would be more appropriate to use the gas density in the derivation. If the density of the gas were used instead of the density of the fluidized bed to describe the buoyancy force, then

$$W_e = \frac{\pi d_p^3}{6} (\rho_p - \rho_f) g \tag{14a}$$

For a single particle at the terminal velocity $u = u_t$, the drag force equals the net force resulting from gravity and buoyancy.

$$F_{ds} = C_d \frac{\rho_f u^2}{2} \frac{\pi d_p^2}{4} = \frac{\pi d_p^3}{6} (\rho_p - \rho_f) g \tag{15}$$

For 100% SAC coated particles, considering the host particles are separated by two guest particles (Figure 9) the cohesive force can be estimated as in Yang et al.,[18] where the attraction between two host particles is neglected compared

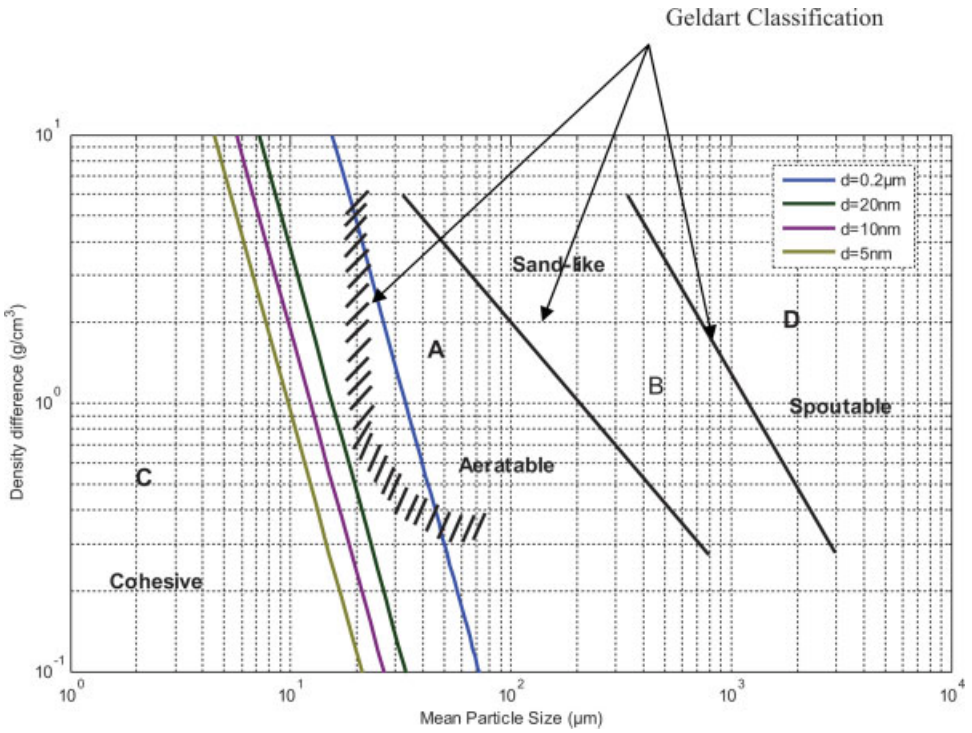

Figure 10. Effect of guest particle size on boundary shift.

[Color figure can be viewed in the online issue, which is available at www.interscience.wiley.com.]

with the adhesion between two guest particles.

$$F_c = \frac{A}{12z_0^2}\frac{d}{2} \tag{16}$$

Substituting the F_d, W_e, and F_c into Eq. 12, letting u approach the terminal velocity of a single particle in Eq. 13, and using Eq. 14a for W_e, the transition equation at the minimum fluidization velocity is

$$\frac{\pi d_p^3}{6}(\rho_p - \rho_f)g(\varepsilon^{-4.8} - 1) = \frac{Ad}{24z_0^2} \tag{17}$$

This equation differs slightly from the one that appears in Qian et al.[7] in that the voidage term is $(\varepsilon^{-4.8} - 1)$ rather than $(\varepsilon^{-4.8} - \varepsilon)$; however for a typical value of $\varepsilon = 0.5$ the numerical difference is negligible. In Eqs. 12–17, d_p is the host particle size, d is the gust particle size, ρ_p is the density of host powder, ρ_f is the gas density, u is the velocity of the particle relative to the gas, and ε is the voidage of the gas–solid flow.

Effect of guest particle size on the Geldart A–Geldart C boundary

The effect of guest particle size on boundary shift is shown in Figure 10 for $A = 10^{-19}$, $\delta = 0.4 \times 10^{-9}$ m, $\varepsilon = 0.5$, and SAC = 100%. Masimilla et al.[20] and Rietema et al.[28] recommend using the size of the asperities rather than the particle size to calculate the adhesion force because most particles have a rough surface with radii of curvature of about 100 nm. Hence Eq. 17, plotted as a straight line in Figure 10 using the typical size of the asperities $d = 200$ nm as the guest particle size, represents the theoretical boundary between Group C and Group A powders. As the guest particle size is reduced, the boundary moves to left, which means that some Group C powders now shift to Group A and can be fluidized individually like Group A particles. It should be noted however, that the fine coated particles may not always fluidize as individual particles. For example, Castellanos et al.[29] performed experiments on the fluidization of toner particles blended with fumed silica ($\rho_p = 1.14$ g/cm^3, $d_p \approx 7.8$, 11.8, 15.4, and 19.1 μm) and found that the toner particles fluidize as agglomerates rather than individual particles by both experimental observation and theoretical calculations. When the coated powders fluidize in form of stable agglomerates, the actual improvement in the fluidization may be under-predicted by the shift shown in Figure 10.

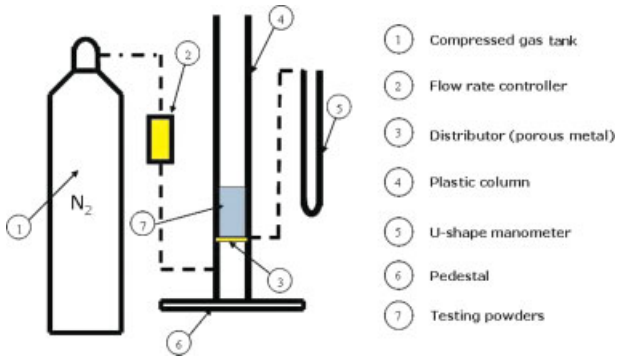

Figure 11. Sketch of the fluidized bed.

[Color figure can be viewed in the online issue, which is available at www.interscience.wiley.com.]

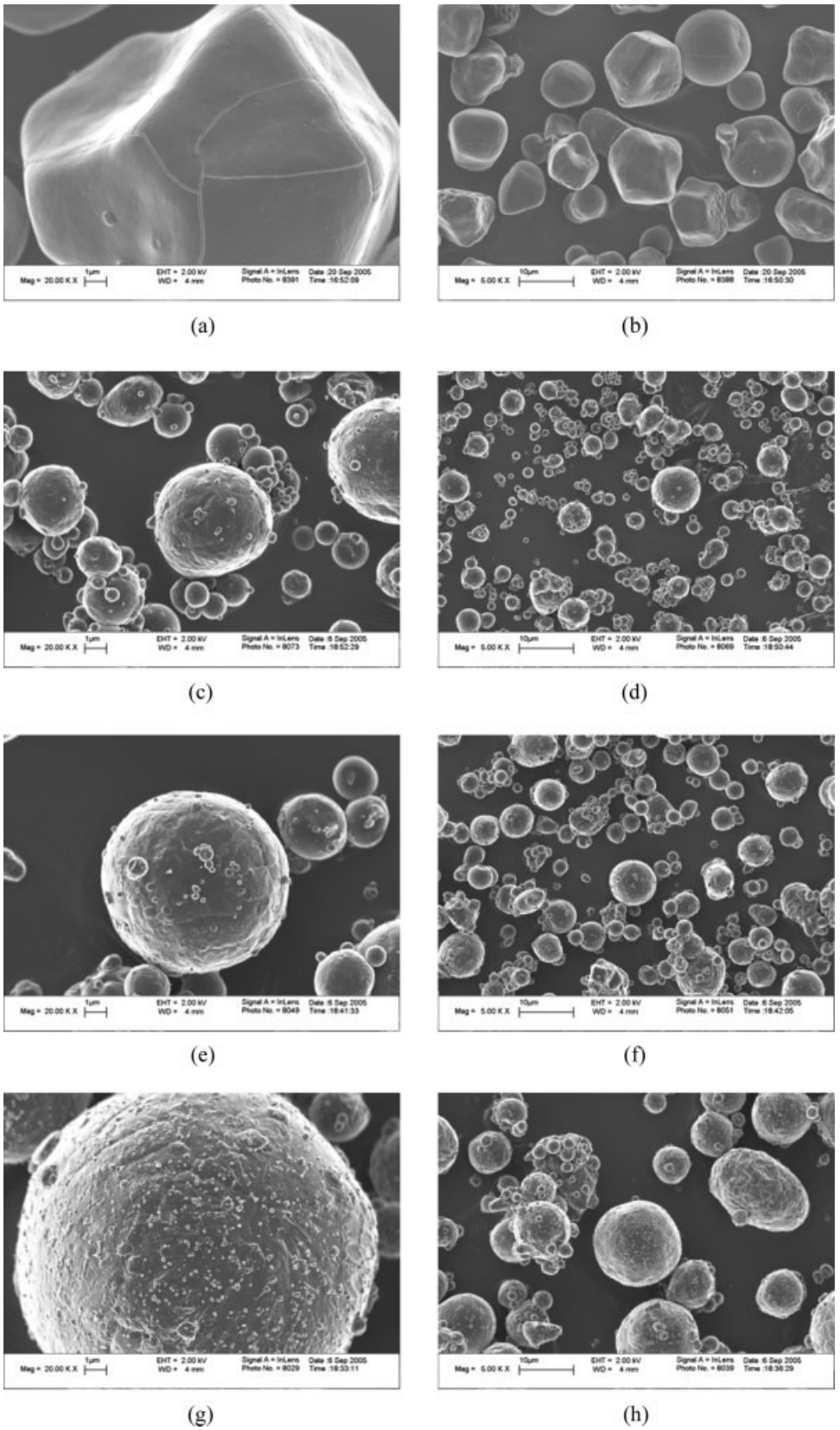

Figure 12. SEM images of uncoated host particles.

(a) Cornstarch (X20,000), (b) Cornstarch (X5,000), (c) 3–4.5-μm aluminum (X)20,000, (d) 3–4.5-μm aluminum (X5,000), (e) 4.5–7-μm aluminum (X20,000), (f) 4.5–7-μm aluminum (X5,000), (g) 10–14-μm aluminum (X20,000), and (h) 10–14-μm aluminum (X5,000).

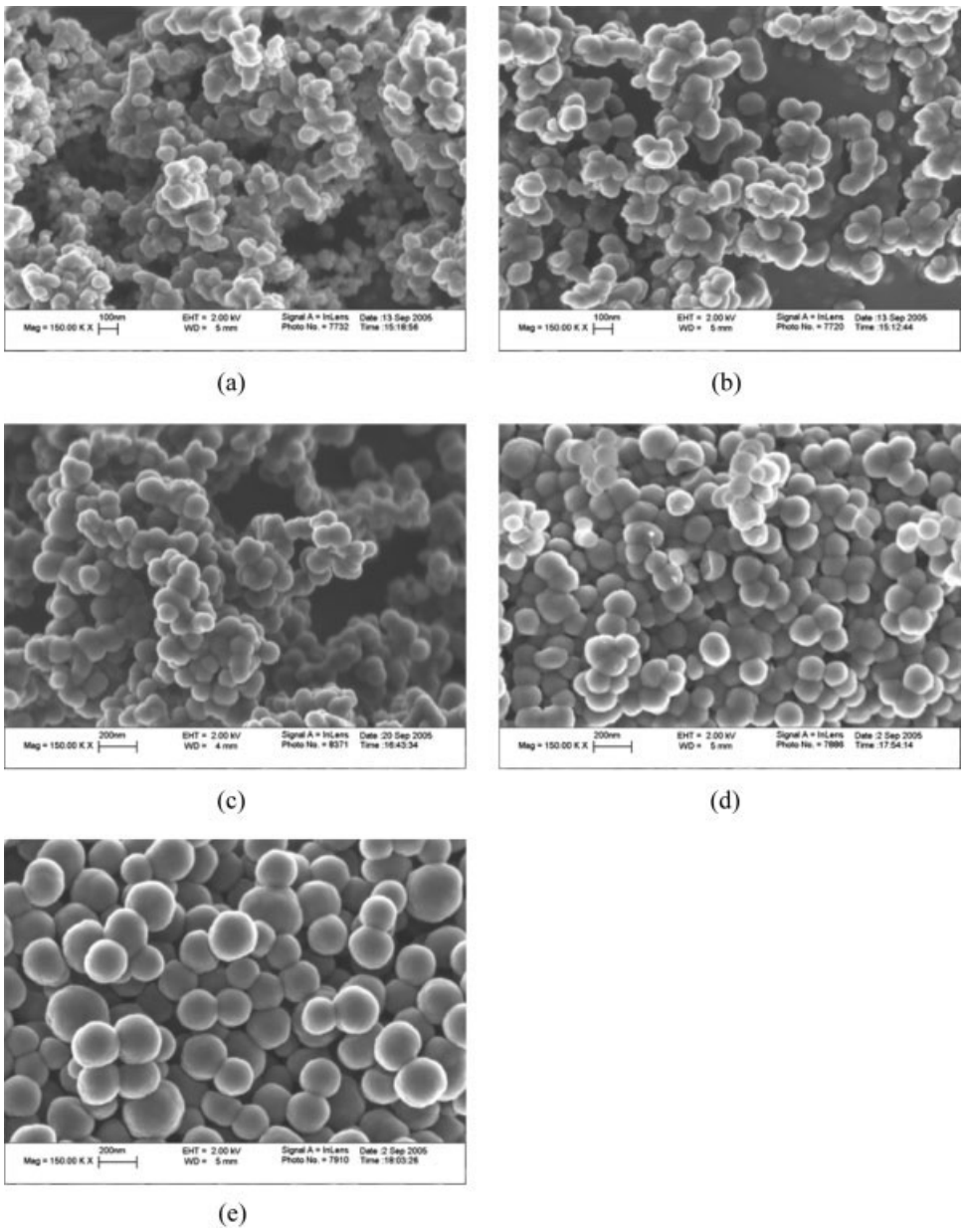

Figure 13. SEM pictures of guest particles.

(a) EH-5 (X 150,000), (b) R972 (X 150,000), (c) OX50 (X 150,000), (d) Lab synthetic 70-nm silica (X 150,000), and (e) Lab synthetic 100-nm silica (X 150,000).

Experimental

To examine the influence of dry particle coating, specifically; the effect of SAC, guest particle size and host particle size on the fluidizability of cohesive powders, a series of fluidization experiments are performed on coated cornstarch and coated aluminum.

Dry particle coating

This series of experiments for dry coating are carried out in a magnetically assisted impaction coater (MAIC).[9,18] In MAIC, the oscillating magnetic field generated by the electric coil is used to accelerate and spin the large magnetic particles mixed with the host and guest particles promoting collisions between the particles and with the walls of the vessel. Since the moving magnetic particles tend to "fluidize" the host and guest powders, dry coating occurs by guest–host particle impaction. The magnetic particles used are barium ferrite particles coated with polyurethane and have a size range from 1.4 to 1.7 mm. The weight ratio of magnets to host and guest particles is 2 to 1. The size and weight ratio of the magnetic particles were chosen on the basis of previous research.[9,18] Unless stated otherwise, the processing time using MAIC was 10 min.

Fluidization

The fluidization experimental setup is shown in Figure 11. The powder sample (100 g for coated cornstarch, 150 g for

Table 1. Properties of Host and Guest Particles

	Size (μm)	Density (Kg/m^3)	Surface Properties
Host particle			
Cornstarch	15	1550	Hydrophilic
Aluminum I	3–4.5	2700	Hydrophilic
Aluminum II	4.5–7	2700	Hydrophilic
Aluminum III	10–14	2700	Hydrophilic
Guest Particle			
EH-5	~7	2650	Hydrophilic
R972	~16	2650	Hydrophobic
OX-50	~40	2650	Hydrophilic
Lab 70-nm silica	~70	2650	Hydrophilic
Lab 100-nm silica	~100	2650	Hydrophilic

Table 2. Weight Ratios and Surface Area Coverage of Cornstarch Coated by MAIC

	Weight Ratio of Guest Particle (%)	Theoretical Surface Area Coverage (%)	Experimental Surface Area Coverage (%)
Cornstarch + R972	0.01	1.17	1.09
	0.025	2.92	2.86
	0.04	4.67	3.85
	0.05	5.84	4.89
	0.08	9.53	8.14
	0.1	11.69	8.50
	0.5	58.44	46.94
	1.0	100.00	89.76

coated aluminum) was held in an acrylic column with an inner diameter of 2 in. and a height of 1 m. A porous metal plate with a 20-μm pore size was used as the gas distributor. A dry nitrogen tank with flow controller was used as the gas source; eliminating any effects of humidity. The pressure drop was measured using a U-shape manometer, which has an accuracy of 0.1-cm water column, connected to the fluidized bed by a plastic tube installed 0.002 m above the distributor. The bed height was measured by a ruler marked on the fluidized bed; the accuracy of the ruler is 0.1 cm. The initial powder bed height ranged from about 7 to 10 cm.

Initially, the tested powder was poured into the fluidized bed and the powder was allowed to settle for 5 min. The gas velocity was increased gradually in increments of 0.1 cm/s until the powder was either homogeneously fluidized for fluidizable powder, or elutriation occurred for nonfluidizable powder. The pressure drop and bed height were recorded for each change in gas velocity. Subsequently, the gas velocity was incrementally decreased by 0.1 cm/s and the pressure drop and bed height were again recorded. Repeated experiments were performed on the settled powder from the previous experiment. Final results of pressure drop and bed height are obtained by averaging results of three experiments.

Materials

Cornstarch and three sizes of aluminum particles were used as host particles for the dry particle coating and subsequent fluidization experiments. The cornstarch supplied by Argo has a size of about 15 μm with a density of about 1550 kg/m^3. As seen in Figures 12a, b, the field emission scanning electron microscope (FESEM) images indicate that the cornstarch particles are irregular individual particles with a smooth surface. The aluminum powders were provided by Alfa Aesar, having a density of 2700 kg/m^3. SEM micrographs of the aluminum powders are shown in Figures 12c–h. All aluminum particles are spherical with rough surfaces.

Five sizes of nano-sized silica were used as guest particles: (1) CAB-O-SIL EH-5 supplied by Cabot with an average size around 7 nm with a chain-like structure (Figure 13a). The untreated silica is hydrophilic in nature. (2) Aerosil R972 silica (shown in Figure 13b) is supplied by Degussa with a specific surface area of 114 m^2/g. A FESEM image shows highly agglomerated particles with an average primary particle size around 16 nm in a chainlike structure. Its surface has been modified by dimethyldichlorosilane to make it hydrophobic. (3) OX-50 silica supplied by Degussa has an average size of about 40 nm (Figure 13c) and is hydrophilic. (4) 70 nm, and (5) 100 nm silica, which are synthesized in our laboratory using the Stober process and are hydrophilic (Figures 13d, e). All the properties of host and guest particles are listed in Table 1.

Results and Discussion

Dry coating of cohesive powders

Dry coating of cornstarch and aluminum powders was conducted in the MAIC device as described above. The weight ratios of the guest and host particles for various coating experiments are listed in Tables 2 and 3. The coating performance was characterized using a FESEM (LEO 1530VP). Table 2 lists the expected SAC based on the amount of R972 fumed silica used with cornstarch at eight different levels. The theoretical SAC is computed based on the assumptions that (1) all the host and guest particles were monosized individual spheres and (2) the guest particles were uniformly coated onto the host particles.

The SEM images of coated cornstarch particles seen in Figure 14 indicate that the R972 fumed silica particles were evenly coated onto cornstarch using MAIC at all SAC levels. No large agglomerates of R972 were detectable in the final coated product, which implies that MAIC is capable of deagglomerating nanosized fumed silica agglomerates and coating it evenly onto the cohesive host particle surface. The evenness of the coating is further verified by plotting the results of the theoretical and experimental SACs against the weight percentage of applied guest particles in Figure 15. The exper-

Table 3. Surface Area Coverage of Cornstarch Coated by MAIC for the Weight Ratios Selected to Achieve 100 % (or Better) Surface Area Coverage

	Weight Ratio of Guest Particles	Experimental Surface Area Coverage (%)	Guest Particle Size (nm)
Cornstarch + EH-5	0.4	100	~7
Cornstarch + R972	1.2	100	~16
Cornstarch + OX-50	2.0	100	~40
Cornstarch + Lab Syn 70-nm silica	3.5	47.86	~70
Cornstarch + Lab Syn 100-nm silica	5.0	49.30	~100

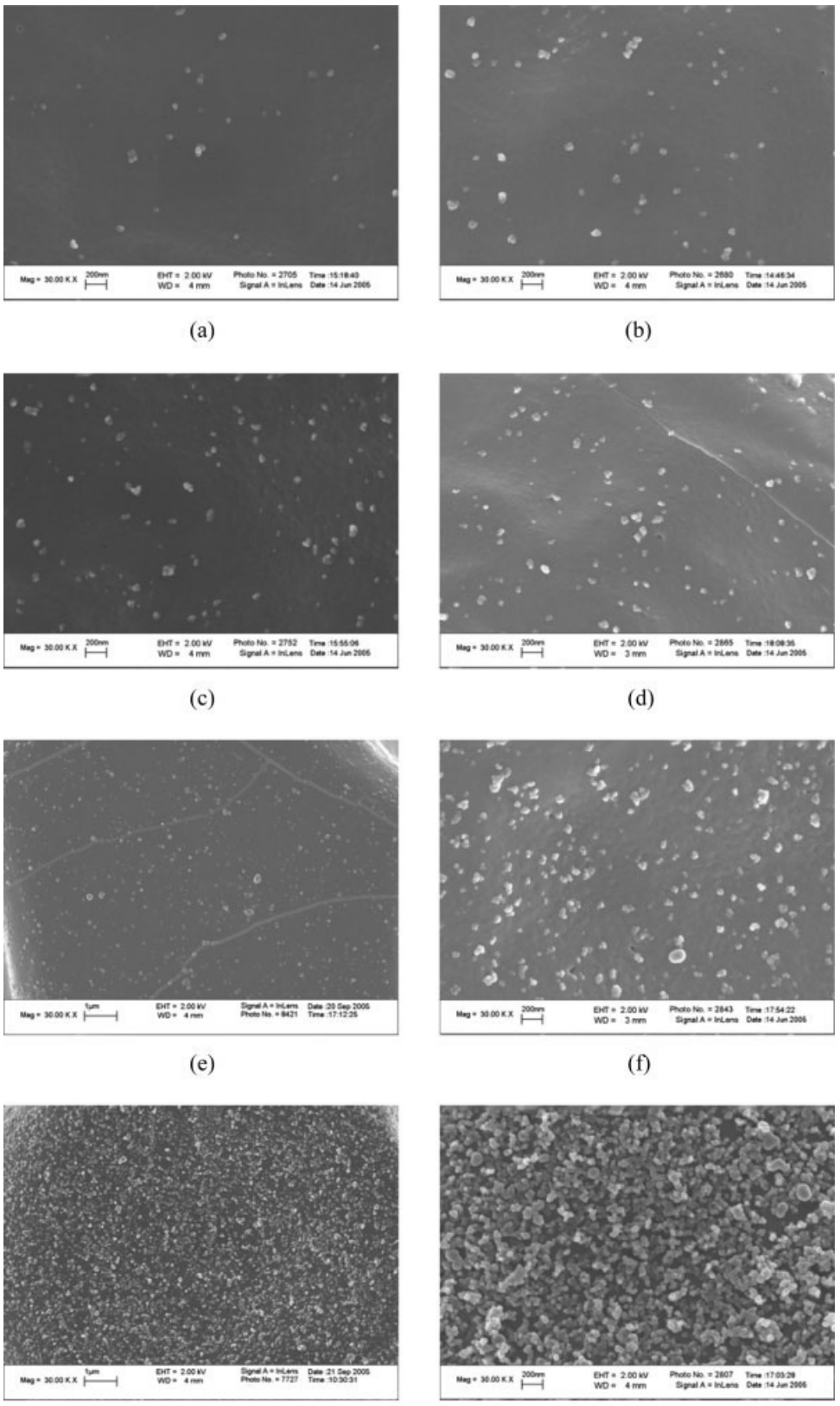

Figure 14. SEM images of Cornstarch coated with R972 with wt % of (a) 0.01 wt % (×30,000), (b) 0.025 wt % (×30,000), (c) 0.04 wt % (×30,000), (d) 0.05 wt % (×30,000) (e) 0.08 wt % (×30,000), (f) 0.1 wt % (×30,000), (g) 0.5 wt % (×30,000), and (h) 1.0 wt % (×30,000).

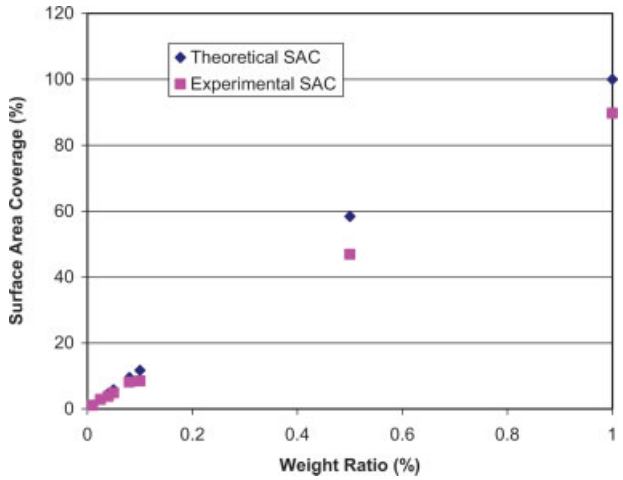

Figure 15. Weight ratio and surface area coverage.

[Color figure can be viewed in the online issue, which is available at www.interscience.wiley.com.]

imental SACs were estimated by the image analysis of randomly selected 12 SEM images for each sample. The method for the image analysis is described in Ref. 18. As listed in Table 2, the values of the theoretical SAC are very close to the corresponding experimental SAC, which demonstrates that the coated nanosized guest particles were well deagglomerated and evenly coated onto the host particles. Both the SEM micrographs and the experimental SAC results indicate that nearly all the fumed silica agglomerates and some of the longer chainlike structures were broken down by MAIC into very small sintered-together chains of perhaps a few primary particles, which were then coated onto the cornstarch host particles. However, in case of higher amounts of guest particles, their deagglomeration and hence their coating coverage is less effective. For example, 1.0 wt % R972 should theoretically achieve 100% coverage, but in practice, the coverage is about 10% less.

Similar coating experiments were performed on cornstarch with different nanosized silica as listed in Table 3. Corresponding SEM pictures of coated cornstarch are shown in Figure 16. As mentioned before, the experimental SAC at 100% is roughly 10% less for R972, thus a larger amount of guest particles were added to ensure that a 100% of SAC is obtained as seen in the third column of Table 3. As listed in Table 3, complete surface coverage was achieved for three commercially available fumed silicas. However, for the lab synthesized silica, only 50% SAC was obtained. This is attributed to the fact that the samples of the synthesized particles included hard agglomerates that were difficult to deagglomerate.

Coating experiments were also conducted for different sizes of aluminum particles with commercially available fumed silica R972. The results are listed in Table 4 and shown in Figure 17. As seen in the figure coating is obtained with nearly 100% SAC for all cases.

The results discussed above indicate that MAIC is capable of coating nanosized particles onto cohesive micron sized host particles evenly, which is demonstrated by the SEM images as well as by the SAC calculations. However, the coating performance is dependant on the properties of the guest particles.

Fluidization of dry coated cohesive powders

Effect of Surface Area Coverage. In the fluidization experiments, eight batches of coated powders listed in Table 2 were examined with the apparatus shown in Figure 11. The measured pressure drop and bed expansion are shown in Figures 18 and 19. For cornstarch coated with 0.01 wt % of R972 (the experimental SAC is 1.09%), typical Group C fluidization phenomena were observed. The reduction in the cohesive forces for low SAC is not sufficient to allow breaking down of large agglomerates by the gas flow and results in channeling and plugging of powders. The pressure drop fluctuates during operation and there is no plateau observed for pressure drop and bed expansion. Slightly fewer fluctuations in pressure drop and bed expansion are detected with 0.025 and 0.04 wt % of R972 coated cornstarch, (corresponding SAC are 2.86 and 3.85%, respectively), but still one cannot observe a clear pressure drop plateau. In addition, the pressure drops are about 10–20% less than the bed weights, which is consistent with the channeling observed during the experiments. Only when the SAC reaches to about 5% with 0.05 wt % of R972, is it possible to obtain a stable plateau of the pressure drop within the bed at the superficial gas velocity larger than 1.0 cm/s. Although a typical Group A particle fluidization behavior is observed, the bed expansion of the coated cohesive particles is observed to be higher than the regular Group A particles.

Increasing the SAC of coated R972 to 8.14% resulted in a more stable fluidization behavior. The measured pressure drop across the bed at high gas superficial velocity approximately equaled the theoretical bed weight per unit cross-sectional area. At the same time, a significant decrease in the minimum fluidization velocity from 1.0 to 0.53 cm/s occurred. During the experiments, the pressure drop was recorded by slowly increasing the superficial gas velocity beyond the value where the pressure drop levels off and then slowly decreasing the superficial gas velocity to zero. The minimum fluidization velocity, plotted in Figure 20, is defined as the superficial gas velocity at which the pressure drop just begins to decrease from plateau as the superficial gas velocity is slowly reduced. Further increasing the SAC to 8.50, 46.94, and even to 89.76% (correspondingly the wt % of coated R972 is increased to 0.1, 0.5, and 1.0 wt %) does not significantly alter the minimum fluidization velocity of the coated cornstarch particles as shown in Figure 20, which also shows error bars based on each experiment repeated three times. In all cases of fluidization, the bed expansion is larger than that of a typical class A powder. Moreover, the expansion for those powders that fluidize well is higher for a lower coating level, implying that bed expansion is less for less cohesive powders. These results are consistent with those obtained by Valverde et al.,[16,17] although for lower theoretical SAC values the SPT described by Valverde et al.[16,17] requires some vibration to initiate the fluidization. In our experiments, vibrations are not employed because the objective is to study the fluidization without any mechanical aids. It is also noted that Valverde et al.[16,17] report incipient fluidization velocity rather than minimum fluidization velocities.

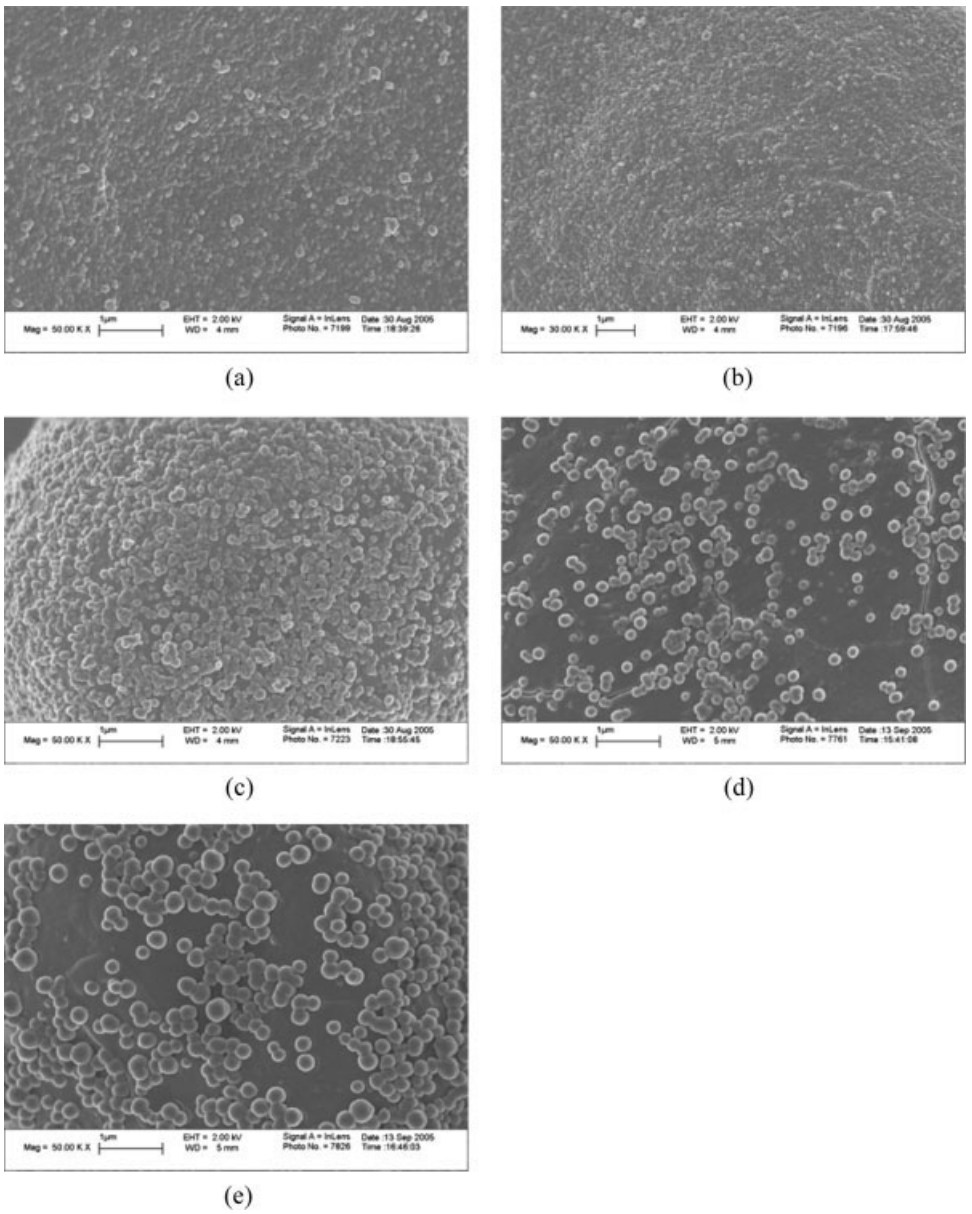

Figure 16. SEM pictures of Cornstarch coated with 100% SAC.

(a) EH-5 (×50,000), (b) R972, (c) OX50 (×50,000), (d) Lab synthetic 70-nm silica (×50,000), and (e) Lab synthetic 100-nm silica (×50,000).

The SAC experimental results for fluidizability agree well with the proposed model for the dependence of cohesion force of coated powders upon SAC; for example, the trend shown in Figure 6 is similar to that shown for the minimum fluidization velocity in Figure 20. As stated before, the proposed model predicts that the cohesion force between particles does not reduce when the SAC is lower than a threshold (~5%); after the SAC reaches a critical value (~10%),

Table 4. Surface Area Coverage of Aluminum Powders Coated by MAIC for the Weight Ratios Selected to Achieve 100 % (or Better) Surface Area Coverage

	Weight Ratio of Guest Particles	Theoretical Surface Area Coverage (%)	Experimental Surface Area Coverage (%)	Host Particle Size (μm)
Aluminum + R972	0.52	100	100	3–4.5
	1.1	100	100	4.5–7
	1.53	100	100	10–14

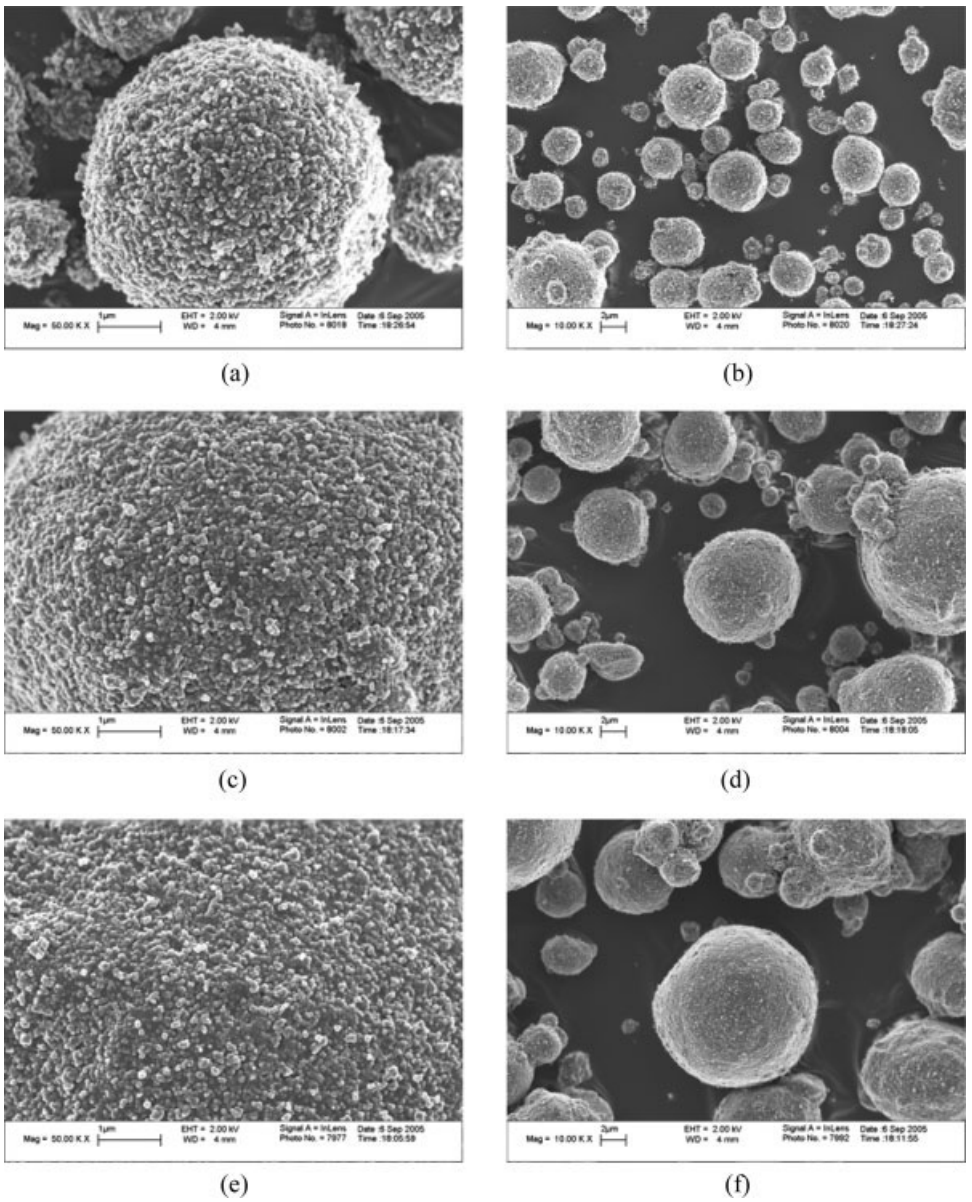

Figure 17. SEM pictures of coated aluminum with R972.

(a) 3–4.5 μm with magnification of 50,000, (b) 3–4.5 μm with magnification of 10,000, (c) 4.5–7 μm with magnification of 50,000, (d) 4.5–7 μm with magnification of 10,000, (e) 10–14 μm with magnification of 50,000, and (f) 10–14 μm with magnification of 10,000.

the cohesion reduces dramatically and reaches a plateau; further increasing the SAC does not produce any additional significant contribution on the cohesion force reduction.

Effect of Guest Particle Size. Another series of fluidization experiment with five different sizes of silica coated cornstarch particles (as listed in Table 3) are conducted to examine the effect of guest particle size on the fluidization behavior. The results indicate that cornstarch host particles coated with 100% SAC EH-5 (7 nm), R972 (16 nm), OX-50 (40 nm), and lab synthesized 70-nm silica can all fluidize stably. The measured pressure drops are shown in Figure 21. It was observed in these and in the previous series of experiments (for cases when coated powders could be fluidized) that the coated powder bed first channeled, and as the superficial air velocity is increased, the pressure drop also increased, and then dropped a little as the channels were destroyed and the powder began to fluidize. A further increase in gas velocity resulted in a pressure drop increase, which subsequently reached a stable plateau as the powders were fully fluidized. Correspondingly, as shown in Figure 22, the bed height is unchanged initially with gas velocity increasing, but then the bed expands as the pressure drop recovers from the slight dip as seen in the figure. On the other hand, cornstarch coated with 100 nm synthesized silica cannot be fluidized. Slugging and channeling were the main characteristics of this powder bed when the gas velocity increased, and the pressure drop did not become stable and nearly no bed expansion was detected.

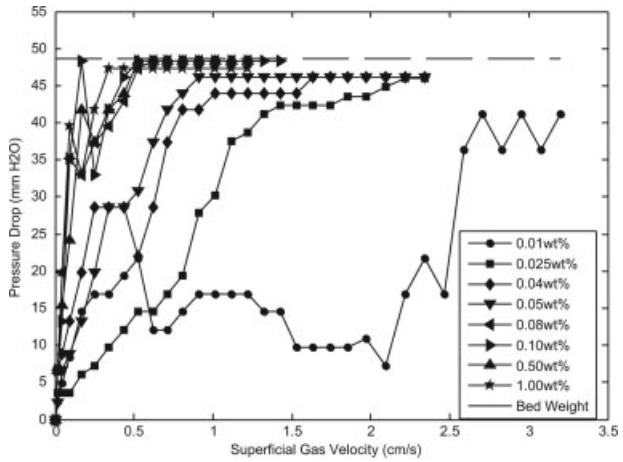

Figure 18. Measured pressure drop of coated Cornstarch with R972.

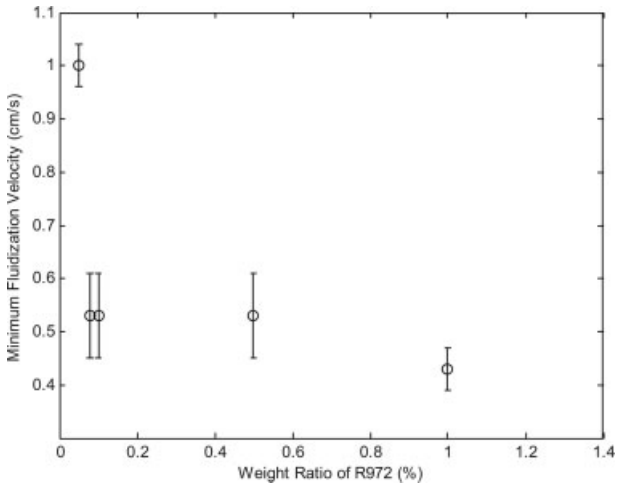

Figure 20. Measured minimum fluidization velocity of coated Cornstarch with R972.

Figure 23 shows the comparison of minimum fluidization velocity of 100% SAC coated cornstarch with EH-5, R972, OX-50, and synthesized 70-nm silica. The plot indicates that the larger the guest particle, the larger the minimum fluidization velocity except for the case of R972, which is a surface modified hydrophobic silica. For 7, 16, 40, and 70-nm silica coated cornstarch particles, the minimum fluidization velocity (U_{mf}) are 0.53, 0.42, 0.80, and 1.10 cm/s, respectively. These results are in general agreement with the trend shown in Figure 7 for cohesion force as a function of the guest particle size.

Effect of Host Particle Size. Most reported results in the literature for unassisted fluidization of cohesive powders through nano-additives are limited to particles of 10 μm and larger. Since dry particle coating can achieve a high degree of coating effectiveness, experiments are conducted with three sizes of Aluminum powders (3–4.5 μm, 4.5–7 μm, and 10–14 μm) used as host particles to examine the capability of the dry coating method to improve fluidization behavior as the host particle size is reduced well below 10 μm. All Aluminum powders were coated with 100% SAC of R972 using MAIC. A fixed value of 100% SAC is used so that the effect of SAC will not influence the results. R972 was used as guest particle because of its better performance in cohesion reduction compared with the other guest particles. Corresponding SEM pictures of uncoated and coated aluminum are shown in Figures 12c–h and 17. The measured pressure drops and bed expansions of coated powders are shown in Figures 24 and 25, respectively. These figures indicate that coated 4.5–7-μm and coated 10–14-μm aluminum can be fluidized, but coated 3–4.5-μm aluminum can not be fluidized. Slugging and channeling were observed when attempting to fluidize coated 3–4.5-μm aluminum even at high velocities. From Figures 24 and 25 we can observe that the minimum fluidization velocity of coated 10–14-μm aluminum is less than that of 4.5–7-μm aluminum. Hence, for the same material with 100% SAC of R972, the larger the host particle size, the better the fluidization behavior. Moreover, dry parti-

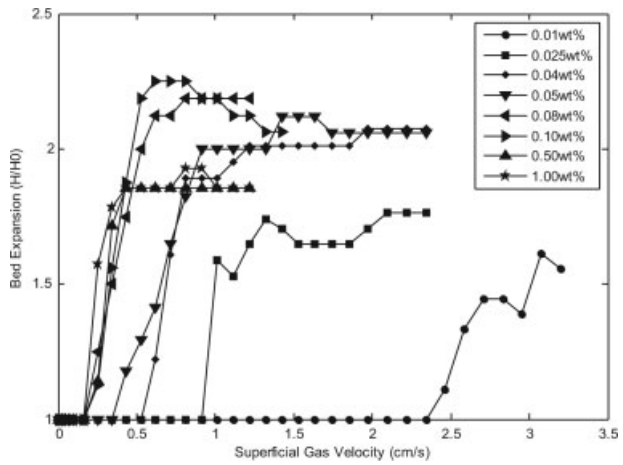

Figure 19. Measured bed expansion of coated Cornstarch with R972.

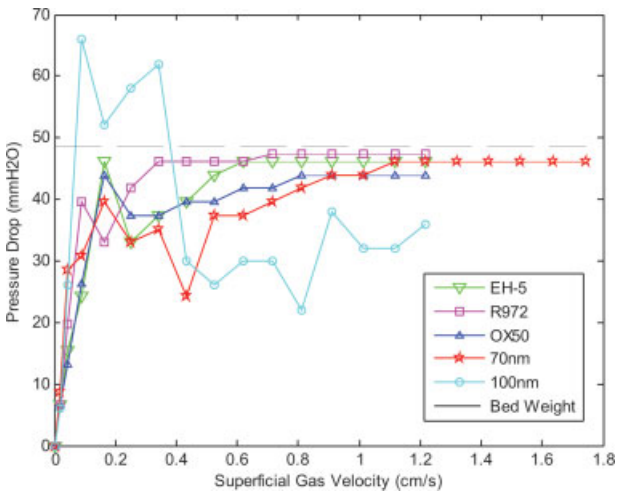

Figure 21. Measured pressure drop of Cornstarch coated with 100% SAC silica.

[Color figure can be viewed in the online issue, which is available at www.interscience.wiley.com.]

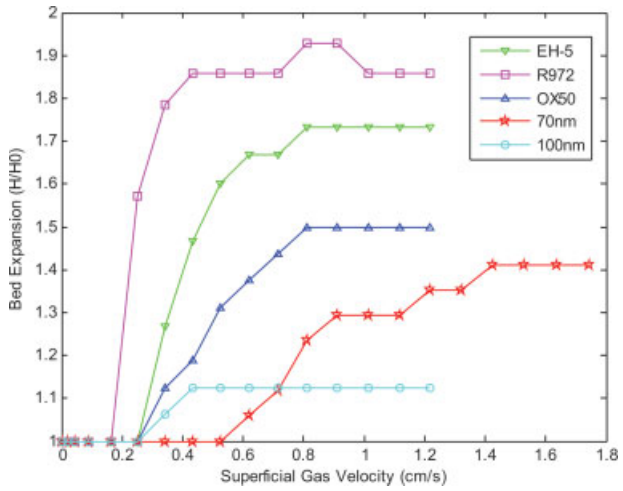

Figure 22. Measured bed expansion of Cornstarch coated with 100% SAC silica.

[Color figure can be viewed in the online issue, which is available at www.interscience.wiley.com.]

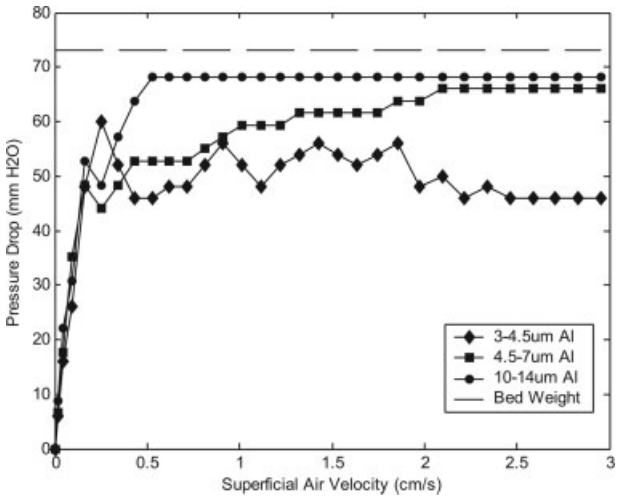

Figure 24. Measured pressure drop of coated aluminum with 100% SAC R972.

cle coating can make 5-μm aluminum behave like Group A powder.

Concluding Remarks

A major objective of this article is to examine the effectiveness of the novel dry particle coating approach in reducing the cohesion force of fine particles and thus improving their fluidization behavior from that of Geldart Group C to Group A. To determine the minimum amount of coating coverage necessary to reduce cohesion, a new model taking into account the effect of SAC as well as the size of the guest particles is derived. Experimental validation of the model was done by dry coating several types of nanosized silica onto the surface of micron-sized cornstarch and aluminum particles. The SEM images of the coated samples indicate that MAIC is able to deagglomerate nanosized guest particles effectively and achieve uniform coating onto cohesive host particles. A comparison of theoretical and experimental SAC values clearly shows the high efficiency of the process. Because of the effectiveness of the dry coating process it is possible to realize an appreciable reduction in cohesion when guest particles as low as 0.05 wt % are used.

Although adhesion force model of Eq. 11, which was introduced previously in Chen et al.,[30] is based on the assumption that the coated nano-particles are individually deagglomerated, the differences in the actual SAC and calculated SAC for cornstarch particles are not significantly different as shown in Table 2. Thus the estimation of critical concentrations will be within the statistical uncertainty of the nature of contact between two coated particles. In Quintanilla et al.,[31] an equation was derived to calculate the SAC of nanosilica on their toner particle surface, assuming the packing fraction of the nanosilica agglomerates for their 8 and 40-nm nominal silica particle diameters, the size of which was determined through SEM imaging. They also employed the expected asperity size (estimated in some cases from the

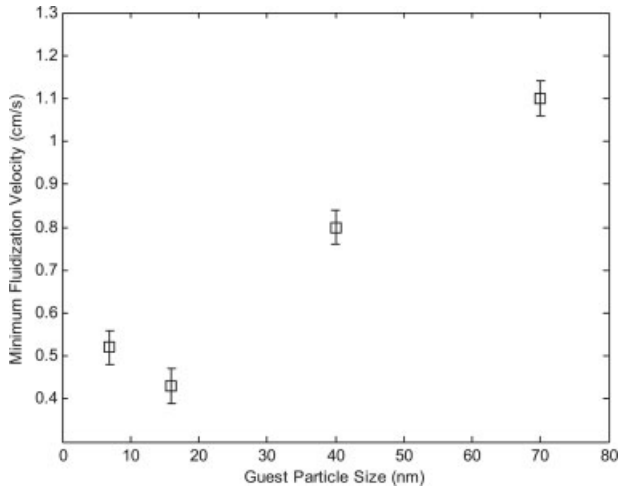

Figure 23. Measured minimum fluidization velocity of Cornstarch coated with 100% SAC silica.

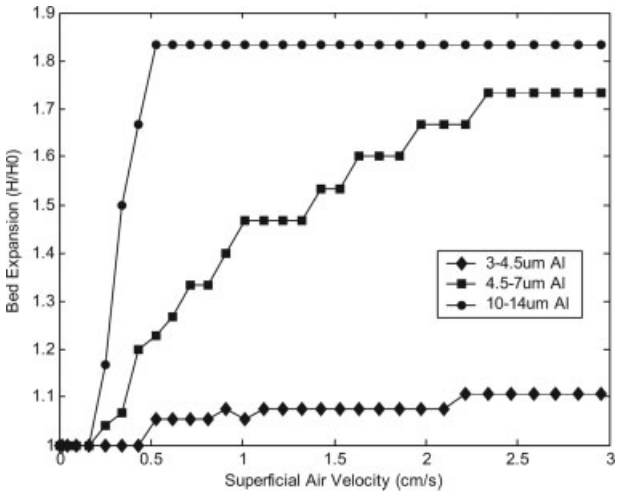

Figure 25. Measured bed expansion of coated aluminum with 100% SAC R972.

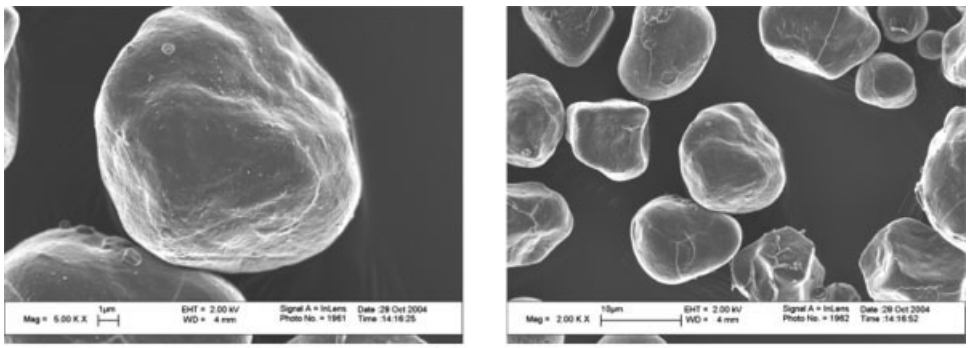

(a) (b)

Figure 26. Individually polymer film coated 15-μm Cornstarch particle in a mini-Glatt at magnification of (a) ×5000 (b) ×2000.

SEM image) rather than the host particle diameter in their calculation. Hence their approach should provide a more accurate estimate of critical concentrations, but would require performing SEM analysis and making assumptions regarding the packing fraction of the nano-agglomerates, whereas our simpler approach does not need SEM analysis. Nonetheless, in practice, either approach should be satisfactory for obtaining a first order estimate of critical concentrations.

A simple derivation shows that by altering the van der Waals forces between the host particles, the boundary between Geldart class A and C will shift to the left so that particles that normally behave as Group C shift to Group A. Fluidization experiments of coated Group C particles indicate that dry particle coating can improve the fluidizability of cohesive powders dramatically, and the coating will transform the behavior of Group C powders to that of Group A powders as predicted theoretically. It was found that the SAC, guest particle size and host particle size all have influence on the fluidization behavior of cohesive powders. Specifically, there exists a critical SAC that is required to make the coated cornstarch fluidize, which is about 5%; the smaller the guest size, the better its effect on improvement in fluidizability, although the improvement is reduced if the guest size becomes much smaller than 10 nm; and if the conditions regarding the SAC and guest size are satisfied, dry particle coating will significantly improve the fluidization of cohesive particles even as small as 5–10 μm.

Once the powders can be fluidized, they can be subsequently processed, for example, they can be film coated or granulated using commercially available devices such as the mini-Glatt fluidized bed processing system. We have successfully granulated and film coated 10–15 μm cornstarch and other powders in a mini-Glatt fluidized bed,[32–34] an example of individually coated cornstarch particles is shown in Figure 26. More detailed results for granulation and coating after dry coating pre-treatment will be presented in a forthcoming article.

Acknowledgments

The authors gratefully acknowledge financial support from the New Jersey Commission of Science and Technology (Award No. 01-2042-007-24) and the National Science Foundation (EEC-0540855). Electron microscopy images were made possible through a National Science Foundation MRI Award (CTS-0116595).

Literature Cited

1. Geldart D. Types of gas fluidization. *Powder Technol*. 1973;7:285–292.
2. Kendall K, Stainton C. Adhesion and aggregation of fine particles. *Powder Technol*. 2001;121:223–229.
3. Herrera CA, Levy EK. Bubbling characteristics of sound-assisted fluidized beds. *Powder Technol*. 2001;119:229–240.
4. Xu C, Zhu J. Parametric study of fine particle fluidization under vibration. *Powder Technol*. 2006;161:135–144.
5. Wang Z, Kwauk M, Li H. Fluidization of fine particles. *Chem Eng Sci*. 1998;53:377–395.
6. Dave R, Wu C, Chaudhuri B, Watano S. Magnetically mediated flow enhancement for controlled powder discharge of cohesive powders. *Powder Technol*. 2000;112:111–125.
7. Qian G, Bagyi I, Burdick IW, Pfeffer R, Shaw H. Gas-solid fluidization in a centrifugal field. *AIChE J*. 2001;47:1022–1034.
8. Alavi S, Caussat B. Experimental study on fluidization of micronic powders. *Powder Technol*. 2005;157:114–120.
9. Pfeffer R, Dave R, Wei D, Ramlakhan M. Synthesis of engineered particulates with tailored properties using dry particle coating. *Powder Technol*. 2001;117:40–67.
10. Lauga C, Chaouki J, Klvana D, Chavarie C. Improvement of the fluidizability of Ni/SiO2 aerogels by reducing interparticle forces. *Powder Technol*. 1991;65:461–468.
11. Rumpf H. *Particle Technology*. London: Chapman and Hall, 1990
12. Xie H. The role of interparticle forces in the fluidization of fine particles. *Powder Technol*. 1997;94:99–108.
13. Hollenbach AM, Peleg AM, Rufner R. Interparticle surface affinity and the bulk properties of conditioned powders. *Powder Technol*. 1983;35:51–62.
14. Kono HO, Hung C, Xi M. The effect of flow conditioners on the tensile strength of cohesive powder structures. *AIChE Symp Ser*. 1989;85:44–48.
15. Dutta A, Dullea LV. A comparative evaluation of negatively and positively charged submicron particles as flow conditioners for a cohesive powder. *AIChE Symp Ser*. 1990;86:26–40.
16. Valverde JM, Castellanos A, Mills P, Quintanilla MAS. Effect of particle size and interparticle force on the fluidization behavior of gas-fluidized bed. *Phys Rev E*. 2003;67:051305.
17. Valverde JM, Ramos A, Castellanos A, Watson PK. The tensile strength of cohesive powders and its relationship to consolidation, free volume and cohesivity. *Powder Technol*. 1998;97:237–245.
18. Yang J, Sliva A, Banerjee A, Dave R, Pfeffer R. Dry particle coating for improving the flowability of cohesive powders. *Powder Technol*. 2005;158:21–33.
19. Podczeck F. *Particle-Particle Adhesion in Pharmaceutical Powder Handling*. London: Imperial College Press, 1998.

20. Massimilla L, Donsi G. Cohesive forces between particles of fluid-bed catalysts. *Powder Technol.* 1976;15:253–260.
21. Rabinovich YI, Adler YJ, Ata A, Singh RK, Moudgil BM. Adhesion between nanoscale rough surface I. Role of asperity geometry. *J Colloid Interface Sci.* 2000;232:10–16.
22. Eichenlaub S, Gelb A, Beaudoin S. Roughness models for particle adhesion. *J Colloid Interface Sci.* 2004;280:289–298.
23. Johnson KL, Kendall K, Roberts AD. Surface energy and the contact of elastic solids. *Proc R Soc London A* 1971;324:301–313.
24. Deryaguin BV, Muller VM, Toporov YP. Effect of contact deformations on the adhesion of particles. *J Colloid Interface Sci* 1975;53:314–325.
25. Mei R, Shang H, Klausner JF, Kallman E. A contact model for the effect of particle coating on improving the flowability of cohesive powders. *Kona* 1997;15:132–141.
26. Nase ST, Vergas WL, Abatan AA, McCarthy JJ. Discrete characterization tools for cohesive granular material. *Powder Technol.* 2001; 116:214–223.
27. Foscolo PU, Gibalaro, LG. A fully predictive criterion for the transition between particulate and aggregative fluidization. *Chem Eng Sci.* 1984;39:1667–1675.
28. Rietema K, Cottaar EJE, Piepers HW. The effect of interparticle forces on the stability of gas-fluidized beds. II. Theoretical derivation of bed elasticity on the basis of Van der Waals forces between powder particles. *Chem Eng Sci.* 1993;48:1687–1697.
29. Castellanos A, Valverde JM, Quintanilla MAS. Aggregation and sedimentation in gas-fluidized beds of cohesive powders. *Phys Rev E.* 2001;64:041304.
30. Chen Y, Yang J, Dave R, Pfeffer R. Fluidization of coated cohesive powders. In: *Proceedings (CD-ROM) of Fifth World Congress on Particle Technology*, Orlando, Florida, April 23–27, 2006:1-7 (Disk-II, Paper 201a).
31. Quintanilla MAS, Valverde JM, Castellanos A. Adhesion force between fine particles with controlled surface properties. *AIChE J* 2006;52:1715–1728.
32. Yang J, Chen Y, Shen Y, Quevedo JA, Dave R, Pfeffer R. Film coating of ultrafine cohesive particles through innovative approaches. In: *Proceedings of AIChE Annual Meeting*, Cincinnati, OH, 2005:8525.
33. Yang J, Chen Y, Dave R, Pfeffer R. Granulation of fine particles using a standard fluidized bed. In: *Fifth World Congress on Particle Technology*, Orlando, Florida, 2006.
34. Dave R, Pfeffer R, Yang J, Chen Y. Dry Coating and Downstream Processing of Cohesive Powders. US Patent 0,053,846, March 8, 2007.

Manuscript received May 14, 2007, and revision received Sept. 24, 2007.